

## Path-integral ground-state Monte Carlo study of two-dimensional solid ${}^4\text{He}$

E. Vitali, M. Rossi, F. Tramonto, D. E. Galli, and L. Reatto

*Dipartimento di Fisica, Università degli Studi di Milano, via Celoria 16, 20133 Milano, Italy*

(Received 9 April 2008; published 13 May 2008)

We have studied a two-dimensional (2D) triangular commensurate crystal of  ${}^4\text{He}$  with the exact  $T=0$  K path-integral ground-state (PIGS) Monte Carlo method. We have projected onto the true ground state two qualitatively different wave functions, a Jastrow-Nosonow wave function and a translationally invariant shadow wave function. The PIGS method passes this hard test of validity and applicability by obtaining the convergence to the same properties, both the diagonal ones as well as the off-diagonal one-body density matrix  $\rho_1$ . Thus, the commensurate 2D  ${}^4\text{He}$  crystal at  $T=0$  K is exactly solved, we find no Bose-Einstein condensation (BEC), and  $\rho_1$  shows a dominant exponential decay in the large distance range. The structure found in  $\rho_1$  is due to virtual vacancy-interstitial pairs and this shows up in the momentum distribution. Our result indicates that BEC in 2D solid  ${}^4\text{He}$  can only arise in the presence of some kind of disorder, either intrinsic or extrinsic.

DOI: [10.1103/PhysRevB.77.180505](https://doi.org/10.1103/PhysRevB.77.180505)

PACS number(s): 67.80.-s

Quantum Monte Carlo methods have provided a very powerful tool in exploring the physics of strongly interacting many-body quantum systems. As far as the properties of Bose fluids and solids are concerned, path-integral Monte Carlo (PIMC) methods were proven to evaluate exact expectation values on the thermal equilibrium state at finite temperature;<sup>1</sup> “exact” means that all systematic errors can be arbitrarily reduced below the statistical errors and the only required input is the interatomic potential. Also at zero temperature, different techniques that are exact in principle are available, such as the Green’s function Monte Carlo<sup>2</sup> (GFMC), the diffusion Monte Carlo<sup>3</sup> (DMC), the reptation Monte Carlo,<sup>4</sup> or the path-integral ground-state<sup>5</sup> (PIGS) methods. However, all such methods rely on variational models for the ground-state wave function (WF) of the system. These variational models play a relevant role in the importance sampling employed by these methods; although, in principle, the final results should not be affected by the particular choice of the trial WF, in practice, the possibility that some bias could survive, especially in systems with complex broken symmetries like in the solid phase, has not been ruled out. Thus, the exact nature of a commensurate crystalline state at  $T=0$  K, if it has Bose-Einstein condensation (BEC) or not, is not known. In this Rapid Communication, we give the exact solution for the commensurate crystalline state of  ${}^4\text{He}$  in two dimensions. In fact, we will show the robustness of the results given by the PIGS method with respect to the choice of the variational WF. We find the same physical properties of the system, within the statistical noise, starting from two radically different WFs. One, a Jastrow-Nosonow<sup>6</sup> WF (JNWF), has built in the crystal lattice via Gaussian localization factors, is not Bose symmetric, and has no BEC. The other, a shadow<sup>7</sup> WF (SWF), is translationally invariant, with crystalline order arising as spontaneous broken symmetry, and it has BEC.<sup>8-10</sup> We have chosen to study this model in two dimensions for different reasons. The reduced dimensionality allows us to study correlations up to much larger distances than in three dimensions, even more than 20 lattice parameters. Fluctuations are expected to be stronger in two dimensions so this is a more stringent test for convergence given the different symmetry properties of

the starting variational WFs. Finally, the two-dimensional (2D) system is a model that is relevant for adsorbed  ${}^4\text{He}$  atoms on a planar substrate like graphite.

With the present study, we address the important question of the supersolid state of matter.<sup>11-16</sup> PIMC computations give strong evidence that in a three-dimensional (3D) commensurate solid  ${}^4\text{He}$  (number of atoms equal to the number of lattice sites), there is no superfluid response and no BEC.<sup>17,18</sup> The PIMC computations are at finite temperature and the lowest  $T$  is of the order of 0.1 K, which is above the experimental transition temperature of crystals of good quality.<sup>12</sup> By computing the density matrix  $\rho_1(\vec{r}, \vec{r}')$  of crystalline  ${}^4\text{He}$  at  $T=0$  K, we find that there is no BEC in a 2D crystal. Preliminary results indicate that this is true also in three dimensions.

In dealing with low temperature properties,  ${}^4\text{He}$  atoms are described as structureless zero-spin bosons, interacting through a realistic two-body potential, which we assume to be the HFDHE2 Aziz potential.<sup>19</sup> The aim of the PIGS method is to improve a variationally optimized trial WF by constructing a path in the Hilbert space of the system that connects the given WF to the true ground state of the system; within this “path,” the correct correlations among the particles arise through the “imaginary time evolution operator”  $e^{-\tau\hat{H}}$ , where  $\hat{H}$  is the Hamiltonian operator. With  $\phi$  being a trial WF with nonzero overlap with the exact ground state  $\psi_0$ , this  $\psi_0$  is obtained as the  $\tau \rightarrow \infty$  limit of  $\psi_\tau = e^{-\tau\hat{H}}\phi$  suitably normalized. This  $\psi_\tau$  can be analytically written by discretizing the path in imaginary time and exploiting the factorization property  $e^{-(\tau_1+\tau_2)\hat{H}} = e^{-\tau_1\hat{H}}e^{-\tau_2\hat{H}}$ . In this way,  $\psi_\tau$  turns out to be expressed in terms of convolution integrals that involve the “imaginary time propagator”  $\langle R|e^{-\delta\tau\hat{H}}|R'\rangle$  for a  $\delta\tau$ , which can be small enough such that very accurate approximants are known.<sup>1,20</sup> This maps the quantum system into a classical system of open polymers.<sup>5</sup> An appealing feature peculiar to the PIGS method is that, in  $\psi_\tau$ , the variational ansatz acts only as a starting point, while the full path in imaginary time is governed by  $e^{-\tau\hat{H}}$ , which depends only on  $\hat{H}$ .

As a trial WF, we used both a JNWF and a SWF. The

JNWF is written as the product of two-body correlations and of Gaussian one-body terms, which localize the particles around the assumed lattice positions.<sup>6</sup> In the SWF, beyond the explicit two-body factors, additional correlations are introduced via auxiliary (shadow) variables, which are integrated out.<sup>7</sup> Nowadays, SWF gives the best variational description of solid and liquid <sup>4</sup>He.<sup>21</sup> In both cases, the variational parameters have been chosen to minimize the expectation value of the Hamiltonian operator. In what follows, we will refer to PIGS when we deal with the projection of the JNWF, and to the shadow path-integral ground state<sup>22</sup> (SPIGS) when we project the SWF.

Because of the Bose statistics obeyed by the atoms, one has, in principle, to account for permutations in the propagator  $\langle R|e^{-\delta\tau\hat{H}}|R'\rangle$ .<sup>1,5</sup> Permutation moves are necessary when the JNWF, which is not Bose symmetric, is used. On the other hand, permutation moves are not necessary whenever the trial WF in  $\psi_\tau$  is already Bose symmetric, as the SWF. However, also for SPIGS, adding permutation moves turns out to be useful in improving the efficiency and the ergodicity of the sampling, mainly in reaching the large-distance range of  $\rho_1$ . In our algorithm, we have introduced two different permutation samplings: cycles of interparticle exchanges and swap moves. The first, which may involve an arbitrary number of particles, are described in detail in Ref. 23. In a PIGS or SPIGS calculation of  $\rho_1(\vec{r}, \vec{r}')$ , the efficiency can be further improved by introducing particular two-particle permutation cycles always involving one of the two positions  $\vec{r}$  and  $\vec{r}'$ : the swap moves.<sup>18</sup> These moves improve very much the efficiency of the computation of  $\rho_1$  and their acceptance rate is remarkably high: in the present 2D system, by using a staging<sup>24</sup> method to sample the free (kinetic) part of the imaginary time propagator, we have found an acceptance rate for this swap move that is nearly 15% in the liquid phase and in the solid phase at densities close to melting.

The 2D <sup>4</sup>He system phase diagram is known from accurate finite temperature PIMC simulations;<sup>25</sup> at zero temperature, both DMC<sup>26</sup> and GFMC<sup>27</sup> were used to investigate its properties mainly for the liquid phase. We have performed SPIGS and PIGS simulations of a 2D <sup>4</sup>He commensurate triangular crystal at  $\rho=0.0765 \text{ \AA}^{-2}$ , slightly above the melting density. In order to control the reliability of our results, we have tested their dependence on both the “projection time”  $\tau$  and the “time step”  $\delta\tau$ . For a fixed value of  $\tau=0.075 \text{ K}^{-1}$ , we have done calculations with  $\delta\tau=1/40, 1/80, 1/160,$  and  $1/320 \text{ K}^{-1}$  and we have used the pair-product approximation<sup>1</sup> for the imaginary time propagator. Reducing  $\delta\tau$  below  $1/40 \text{ K}^{-1}$  affects only marginally the results; for example, by using  $1/320 \text{ K}^{-1}$ , the obtained energy is only 1% lower than the one with  $1/40 \text{ K}^{-1}$ . So we have adopted in most of the computations  $\delta\tau=1/40 \text{ K}^{-1}$  as a reasonable compromise between accuracy and computational effort. These tests provide also a robust check of the ergodicity of the sampling algorithm since a lower value of  $\delta\tau$  for a given  $\tau$  means a bigger number of small time projections (convolution integrals) so that one is dealing with polymers of increasing length. We have then increased  $\tau$  until convergence in the results has been achieved.

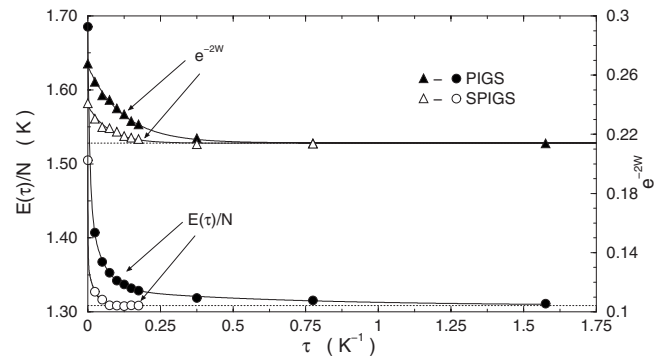


FIG. 1. Energy per particle  $E/N$  and Debye-Waller factor  $e^{-2W}$  as functions of the projection time  $\tau$  obtained from PIGS and SPIGS for a commensurate 2D <sup>4</sup>He crystal with  $N=120$  particles at  $\rho=0.0765 \text{ \AA}^{-2}$ . Error bars are smaller than the used symbols. The dotted lines indicate the convergence values  $\epsilon_0=1.308 \pm 0.002 \text{ K}$  and  $e^{-2W}=0.214 \pm 0.002$ ; solid lines are exponential fits to guide the eye.

Diagonal properties, such as energy, have been computed in a box that hosts  $N=120$  particles with periodic boundary conditions. In Fig. 1, we give the energy per particle as a function of  $\tau$  both for SPIGS and PIGS: at  $\tau=0.075 \text{ K}^{-1}$ , the SPIGS result is already converged to the value  $E/N=1.309 \pm 0.002 \text{ K}$ , while with the PIGS, one reaches convergence at  $\tau=1.575 \text{ K}^{-1}$ , where the energy takes the value  $E/N=1.311 \pm 0.002 \text{ K}$ . The potential energy values are, respectively,  $-11.053 \pm 0.004 \text{ K}$  and  $-11.048 \pm 0.006 \text{ K}$ . From Fig. 1, it is evident that the true ground-state value is reached much more quickly (i.e., with a lower number of small-time projections) with SPIGS. The overlap between the trial WF and the true ground state plays a crucial role in the convergence: a large overlap ensures that  $\psi_\tau$  is a good approximation even for not too large  $\tau$ . It was shown<sup>28</sup> that  $|\langle \psi_0 | \phi \rangle|^2 = (e^{-\gamma})^N$ , where  $\gamma$  corresponds to the area of the region between  $E(\tau)/N$  and its convergence value  $\epsilon_0$ . From our results,  $e^{-\gamma}$  turns out to be 99.8% for the SWF and 97.9% for the JNWF. From the peaks in the static structure factor, we have extracted the Debye-Waller factor; we have found that both SPIGS and PIGS converge to the same value  $e^{-2W}=0.214 \pm 0.002$  (Fig. 1) and, as in the energy case, SPIGS shows a faster convergence.

In order to study whether the 2D commensurate solid <sup>4</sup>He has BEC, we have computed the one-body density matrix  $\rho_1(\vec{r}, \vec{r}')$ . A nonzero limit of  $\rho_1$  for  $|\vec{r}-\vec{r}'| \rightarrow \infty$  implies BEC, and the Fourier transformation of  $\rho_1$  gives the momentum distribution  $n_{\vec{r}}$ . We have computed  $\rho_1$  in a 2D commensurate crystal at  $\rho=0.0765 \text{ \AA}^{-2}$  in a simulation box with  $N=240$  particles (this allows us to explore distances up to about  $39 \text{ \AA}$ ). In our calculations, we have sampled  $\rho_1(\vec{r}, \vec{r}')$  in two different ways. In the first one, we force  $\vec{r}-\vec{r}'$  to lie on a nearest-neighbor direction, while in the second,  $\vec{r}$  and  $\vec{r}'$  are allowed to explore the full plane; we have found perfectly consistent results. In Fig. 2, we show the convergence of  $\rho_1$  computed along the nearest-neighbor direction with SPIGS and PIGS for increasing projection time. The  $\rho_1$  given by SWF has a nonzero limit at large distance, i.e., there is BEC as in three dimensions.<sup>9</sup> When projecting from SWF, the

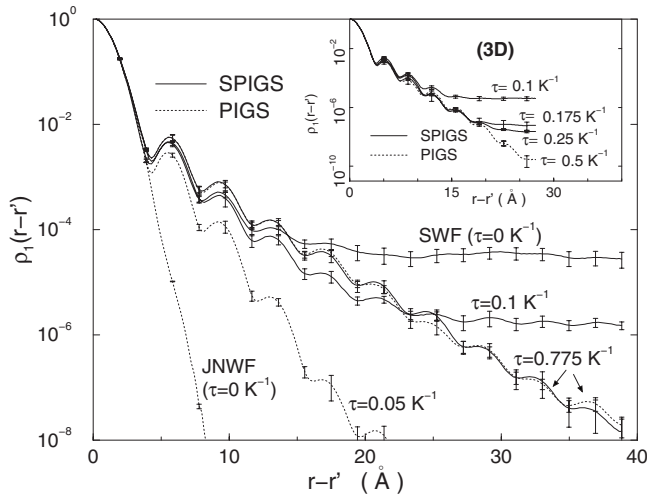


FIG. 2. One-body density matrix  $\rho_1(\vec{r}-\vec{r}')$  computed along the nearest-neighbor direction in a 2D commensurate  $^4\text{He}$  crystal at the density  $\rho=0.0765 \text{ \AA}^{-2}$  for different  $\tau$  values. Notice the completely different behavior for the two initial WFs and the convergence to the same  $\rho_1$ . The inset shows, with the same notation, preliminary results in a 3D commensurate hcp  $^4\text{He}$  crystal at  $\rho=0.0293 \text{ \AA}^{-3}$ .

large distance plateau decreases for increasing  $\tau$  until, at  $\tau=0.775 \text{ K}^{-1}$ , it disappears up to the distance allowed by the simulation box. At convergence,  $\rho_1$  displays an exponential decay, with a correlation length  $\lambda \approx 2.75 \text{ \AA}$ , with a superimposed small modulation reflecting the crystal symmetry. The  $\rho_1$  given by the JNWF is essentially a Gaussian. Under projection, exchanges among the atoms greatly extended the range of  $\rho_1$ . Convergence to the same result for  $\tau=0.775 \text{ K}^{-1}$  means that we have obtained the exact result for  $\rho_1$  and that no BEC is present in the system. Similar conclusions are reached also from the computation of  $\rho_1$  in the whole plane. In Fig. 3(a), we show  $\rho_1$  obtained both with SPIGS ( $x-x' > 0$  range) and PIGS ( $x-x' < 0$  range) with the projection time  $\tau=0.775 \text{ K}^{-1}$ . Again, the results are indistinguishable within the statistical error. We have looked also for finite size effects by considering a system at the same density but with different particle numbers ( $N=180, 240,$  and  $480$ ) and we have found no appreciable differences. With PIGS, we have studied  $\rho_1$  up to a distance of about  $60 \text{ \AA}$ , finding the same exponential decay.

We conclude that a 2D commensurate  $^4\text{He}$  crystal has no BEC or, more precisely, the condensate fraction, if any, is below  $10^{-8}$ . We notice that exchange processes are rather significant in the system, so that the range of  $\rho_1$  is significantly larger than the size of the unit cell. This manifests itself in the momentum distribution [Fig. 3(b)] as a deviation  $\Delta n_{\vec{k}}$  of  $n_{\vec{k}}$  from the Gaussian corresponding to the kinetic energy. There is an excess of particles at low momenta up to  $k=1.2 \text{ \AA}^{-1}$ , whereas there is a deficit in the  $k$ -space region at around  $k=1.6 \text{ \AA}^{-1}$ . The positions of the bumps of  $\rho_1$  over the exponential decay suggest that the extension of  $\rho_1$  beyond the unit cell can be interpreted as a signal of the appearance of vacancy-interstitial pairs (VIPs): their position with respect to the origin ( $\vec{r}=\vec{r}'$ ) corresponds to interstitial positions, whereas the distance between the positions of two neighboring bumps is equal to the lattice parameter. In the

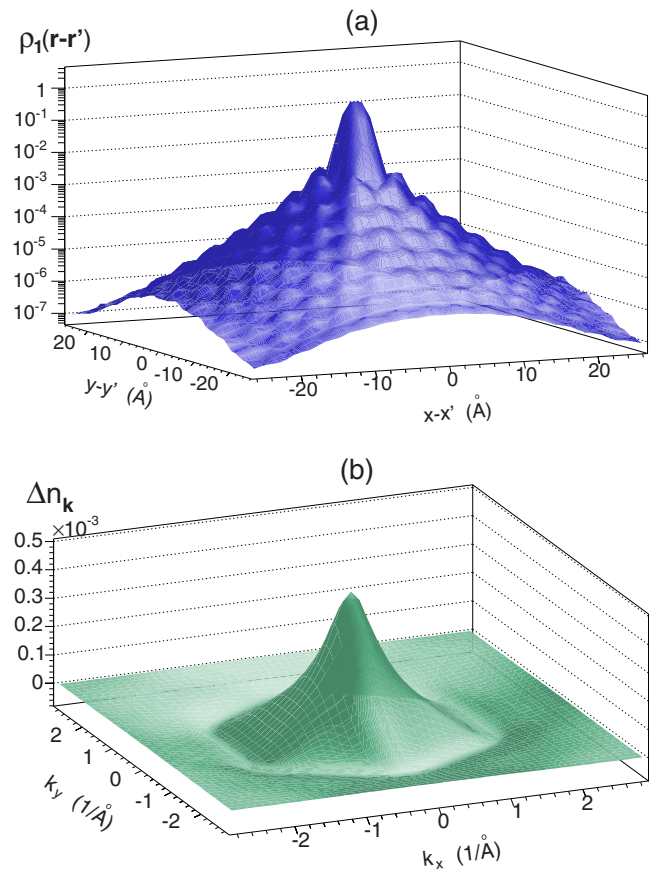


FIG. 3. (Color online) (a) One-body density matrix  $\rho_1(\vec{r}-\vec{r}')$  computed in a 2D commensurate  $^4\text{He}$  crystal with 224 particles at the density  $\rho=0.0765 \text{ \AA}^{-2}$ ; in the  $x-x' > 0$  ( $x-x' < 0$ ) range, the SPIGS (PIGS) results are displayed. (b) Deviation of the momentum distribution  $\Delta n_{\vec{k}}$  from the Gaussian distribution  $n_{\vec{k}} = \frac{2m\hbar^2}{m(T)} \exp(-\frac{\hbar^2 \vec{k}^2}{2m(T)})$ , obtained by Fourier transforming the difference between the SPIGS  $\rho_1$  and the Gaussian distribution corresponding to the kinetic energy  $\langle T \rangle$ .

case of the SWF, these VIPs are unbound, allowing for a finite BEC,<sup>9</sup> whereas these pairs are bound in the exact  $\psi_0$ . This might be due to the presence of some long range correlations in  $\psi_0$ , possibly caused by the zero-point motion of transverse phonons, which are absent in the SWF. Since the ground-state WF reflects the zero-point motion of any excitation in the system,<sup>29</sup> it is tempting to suggest that the evidence of VIPs in  $\rho_1$  is the manifestation of a different kind of excitation in the quantum solid beyond the phonon excitations.

In the inset of Fig. 2, we show  $\rho_1$  computed along the nearest-neighbor direction at  $T=0 \text{ K}$  in the 3D commensurate  $^4\text{He}$  hcp crystal near the melting density in a box with  $N=540$  atoms: by increasing the projection time, we find that the  $\rho_1$  computed with SPIGS and with PIGS coincide within the statistical noise up to about  $20 \text{ \AA}$ , which is the largest distance studied with the PIMC method.<sup>30</sup> At larger distances, SPIGS and PIGS disagree, but we need to verify the convergence of both methods by using a larger value of  $\tau$ ; this is a major numerical task due to the very large number of degrees of freedom.

Experimentally, it is established that defects and  $^3\text{He}$  im-



purities have an important role on the nonclassical rotational inertia (NCRI) of  $^4\text{He}$  crystal, and dislocations are suspected to have a relevant role,<sup>12</sup> at least in the case of good quality crystals. It is an open question what happens in a solid with less and less defects: Will any NCRI effect go away? Our result suggests that it should go away unless some disorder is present even in the ground state as an intrinsic property of  $\psi_0$ . A key question is therefore to establish whether zero-point defects are present in the ground state of a quantum solid. We believe that the presence of zero-point defects in solid  $^4\text{He}$  is still an open question.<sup>31</sup> Since a SWF, which has BEC, is the exact ground state of a suitable Hamiltonian, the interesting question is for which class of interatomic potentials does the commensurate crystal have BEC and supersolidity?

The convergence in the results obtained starting from radically different WFs supplies strong evidence for the ab-

sence of any variational bias in the PIGS method; thus, an exact solution for 2D solid  $^4\text{He}$  at  $T=0$  K has been obtained and we find that BEC does not occur. Moreover, even if not shown in this Rapid Communication, the PIGS method has passed another strong test of validity and applicability: we have studied diagonal properties, such as the static structure factor and the radial distribution function, in the solid phase of  $^4\text{He}$  and obtained their convergence by projecting a simple Jastrow WF, which has just minimal information on the short range correlations and displays no crystalline order at the considered density.

This work was supported by the INFN Parallel Computing Initiative, by the Supercomputing facilities of CILEA, and by the Mathematics Department “F. Enriques” of the Università degli Studi di Milano.

- 
- <sup>1</sup>D. M. Ceperley, *Rev. Mod. Phys.* **67**, 279 (1995).  
<sup>2</sup>P. A. Whitlock, D. M. Ceperley, G. V. Chester, and M. H. Kalos, *Phys. Rev. B* **19**, 5598 (1979).  
<sup>3</sup>M. H. Kalos, D. Levesque, and L. Verlet, *Phys. Rev. A* **9**, 2178 (1974).  
<sup>4</sup>S. Baroni and S. Moroni, *Phys. Rev. Lett.* **82**, 4745 (1999).  
<sup>5</sup>A. Sarsa, K. E. Schmidt, and W. R. Magro, *J. Chem. Phys.* **113**, 1366 (2000).  
<sup>6</sup>L. H. Nosanow, *Phys. Rev. Lett.* **13**, 270 (1964).  
<sup>7</sup>S. A. Vitiello, K. Runge, and M. H. Kalos, *Phys. Rev. Lett.* **60**, 1970 (1988).  
<sup>8</sup>L. Reatto and G. L. Masserini, *Phys. Rev. B* **38**, 4516 (1988).  
<sup>9</sup>D. E. Galli, M. Rossi, and L. Reatto, *Phys. Rev. B* **71**, 140506(R) (2005).  
<sup>10</sup>D. E. Galli and L. Reatto, *J. Low Temp. Phys.* **124**, 197 (2001).  
<sup>11</sup>E. Kim and M. H. W. Chan, *Science* **305**, 1941 (2004); *Nature (London)* **427**, 225 (2004); *J. Low Temp. Phys.* **138**, 859 (2005); *Phys. Rev. Lett.* **97**, 115302 (2006).  
<sup>12</sup>X. Lin, A. C. Clark, and M. H. W. Chan, *Nature (London)* **449**, 1025 (2007).  
<sup>13</sup>Anne Sophie C. Rittner and J. D. Reppy, *Phys. Rev. Lett.* **97**, 165301 (2006).  
<sup>14</sup>M. Kondo, S. Takada, Y. Shibayama, and K. Shirahama, *J. Low Temp. Phys.* **148**, 695 (2007).  
<sup>15</sup>A. Penzev, Y. Yasuta, and M. Kubota, *J. Low Temp. Phys.* **148**, 677 (2007).  
<sup>16</sup>Y. Aoki, J. C. Graves, and H. Kojima, *Phys. Rev. Lett.* **99**, 015301 (2007).  
<sup>17</sup>M. Boninsegni, N. V. Prokof'ev, and B. V. Svistunov, *Phys. Rev. Lett.* **96**, 105301 (2006); B. K. Clark and D. M. Ceperley, *ibid.* **96**, 105302 (2006).  
<sup>18</sup>M. Boninsegni, Nikolay Prokofev-, and B. Svistunov, *Phys. Rev. Lett.* **96**, 070601 (2006); *Phys. Rev. E* **74**, 036701 (2006).  
<sup>19</sup>R. A. Aziz, V. P. S. Nain, J. S. Carley, W. L. Taylor, and G. T. McConville, *J. Chem. Phys.* **70**, 4330 (1979).  
<sup>20</sup>M. Suzuki, *Phys. Lett. A* **201**, 425 (1995).  
<sup>21</sup>S. Moroni, D. E. Galli, S. Fantoni, and L. Reatto, *Phys. Rev. B* **58**, 909 (1998).  
<sup>22</sup>D. E. Galli and L. Reatto, *Mol. Phys.* **101**, 1697 (2003); *J. Low Temp. Phys.* **136**, 343 (2004).  
<sup>23</sup>M. Boninsegni, *J. Low Temp. Phys.* **141**, 27 (2005).  
<sup>24</sup>E. L. Pollock and D. M. Ceperley, *Phys. Rev. B* **30**, 2555 (1984).  
<sup>25</sup>M. C. Gordillo and D. M. Ceperley, *Phys. Rev. B* **58**, 6447 (1998).  
<sup>26</sup>S. Giorgini, J. Boronat, and J. Casulleras, *Phys. Rev. B* **54**, 6099 (1996).  
<sup>27</sup>P. A. Whitlock, G. V. Chester, and M. H. Kalos, *Phys. Rev. B* **38**, 2418 (1988).  
<sup>28</sup>C. Mora and X. Waintal, *Phys. Rev. Lett.* **99**, 030403 (2007).  
<sup>29</sup>L. Reatto and G. V. Chester, *Phys. Rev.* **155**, 88 (1967).  
<sup>30</sup>N. V. Prokof'ev, *Adv. Phys.* **56**, 381 (2007).  
<sup>31</sup>D. E. Galli and L. Reatto, *Phys. Rev. Lett.* **96**, 165301 (2006).